

Chapter 5

Harmonic Stability of Grid

Connected Wind Energy Source - A Case Study

5.1 Introduction

Today, the world's energy supply is, to a great extent, based on fossil energizes and atomic force. These wellsprings of energy will not keep going forever and have demonstrated to be one of the primary driver of our ecological issues. In the long haul renewable energy such as wind energy, will essentially rule the world's energy supply framework. Energy requirement everywhere throughout the world is increasing day by day. Keeping in mind the end goal to take care of the demand, ordinary way to deal with the energy requirements must be reoriented toward energy systems, taking into account renewable energy and energy proficiency, which will make it conceivable to address social, monetary, and ecological concerns all the while.

In past years, with rapid development in power electronic devices and technology, the nonlinear loads such as diodes, rectifiers, electric arc furnaces, have been increasing at phenomenal rate. These nonlinear loads inject substantial amount of harmonics into power system and are real cause of poor quality of power [352]. Power Quality problems have been associated with security, stability, economic and reliable operation of power system as a whole and system equipment(s). Power Quality has become an interesting motive in the research field of reactive power compensation and electrical power quality

control. This work is dedicated to one such problem observed in small Wind Power Plant in India. In case of renewable source, when full scale inverter is integrated into the conventional grid, the variable power flow and mode of operation has been influencing the Power Quality of the Power System [353].

Power Quality is an essential aspect for reliable operation of power grid including inverter based wind power generation. This chapter is based on real time problem of harmonic injection and resonance in power network with 5MW Wind Power Plant. The Wind Plant has 10 WTG of Type-IV (Full Scale Converter), each of 500KW rating. WTG has been connected to 33 kV bus through transformer. Wind Power has been evacuated from 220 KV Substation via 4 km Cable of 33 kV. It was observed that due to injection of harmonics and resonance at specific frequency, several inverters were tripping above certain generation level. Voltage fluctuation has also been observed for small duration of time. This chapter has been devoted to address the real time issue faced in the field. The complete case study is presented here, starting from problem description to the deployment of solution.

5.2 Network Description

In the network, there are ten number of Wind inverters on 0.265 kV side. The voltage has been raised using 0.265/1.1 kV (500 KVA, Dy11, 5%) step up transformer and connected to 1.1 kV bus via 0.08 kM cable. The 1.1 kV buses has been connected to 33 kV bus (PCC) via 1.1/33 kV (2.5MVA, Dyn11, 6.35 %) step up transformer with the help of 0.003 km cable. At 33 kV PCC, voltage level is further stepped up using 33/220 kV (7.5 MVA, YnYn0, 10 %) transformer, and finally evacuated from 220 kV Bus

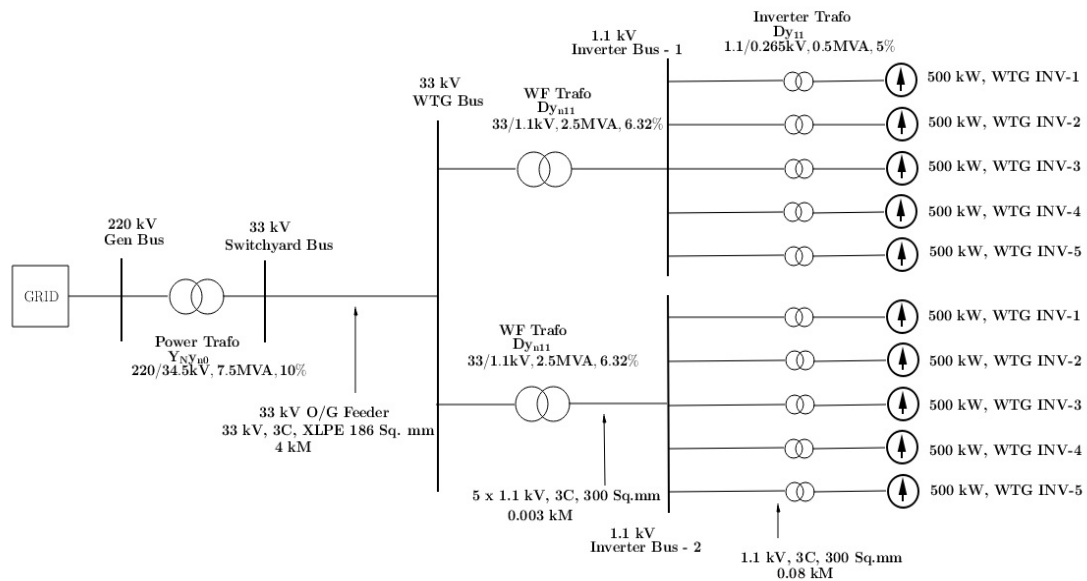


Figure 5.1: System Network

5.3 Problem Description

One of the most important factor while integrating WTG into grid is the harmonics level, measured at PCC. It is mostly caused by non-linear power electronic loads connected to the grid. Power electronics converters are also generating harmonics. So, connecting WTG to power system induce additional stress in power system. To know the harmonic level, Total Harmonic Distortion (THD) is used as a measure to know the extent of harmonic distortion in any network. Based on harmonic level, essential steps should be taken towards mitigation of harmonics and ensure better quality of power [354].

A small wind power plant in the state of Uttar Pradesh was facing typical problem of frequency inverter tripping under overvoltage. The 5 MW Wind power plant consists of 10 inverters, each of 500 KW. When run in parallel, each set of 5 inverters (under the same 2.5 MVA transformer) is able to run stable up to around 2.3 MW power. When the wind speed exceeds to 8-9 m/s and plant reaches exceeds 2.3 MW, all of sudden many inverters were tripping. The error logged was Line Overvoltage fast. This indicates that the line voltage (265V nominal) has exceeded 120 % for more than 160 milliseconds. However, the error was clearing immediately and the inverter starts working in normal condition. Also, it was observed that, just before tripping, the inverters were giving

an unhealthy sound. This sound indicates that there had been a change in the IGBTs switching frequency. During this period, there was a surge in both 1.1 kV and 33 kV side. Due to this problem, it was not possible to utilize the full capacity of wind turbines.

5.4 Methodology

To know the exact nature of problem, first the site was visited and detail information and system related data were collected. For the analysis of the problem, the following steps were followed.

1. Collection of System data and technical discussion with plant team.
2. On Site Power Quality Measurements using Fluke-435 Power Analyser and collection of other relevant data. (Power Quality measurement was done at wind power plant, to find of the harmonic levels and spectrum. Also, the fault history was pulled out from the inverter tripping record. Then, the power level at the time of tripping was also noted. Finally, all this information was related to draw out the reason for tripping.)
3. Modelling of components, like Transformer, Cable, Transmission Lines, inverters etc... [355] [356] [357]. For modelling, transformer, transmission line and cable are represented by their positive sequence impedance and admittance. The inverter is modelled as the current source with very high internal impedance.
4. Frequency scan of network using EMTP-RV 3.5.
5. Fine tuning of network parameters to match the result of frequency scan and on-site measurements.
6. Formulation of Differential Algebraic Equations (DAE)
7. Transformation of DAE in to State-Space form.
8. Eigenvalue analysis of Stat-Space Matrix
9. Sensitivity Analysis using eigenvectors
10. Identifying proper location for filter installation in the given Power System.

11. Comparison of eigenvalue analysis with the frequency scan of network using EMTP-RV version 3.5 [358]
12. Design of harmonic filter(s) to comply with IEEE 519-2014 harmonic distortion limits [352]. In this step, the filter is designed iteratively. After the design of filter, the simulation is done again and THD limits are checked according to IEEE 519-2014. If distortion level, after inclusion of filter in network, is under the IEEE 519-2014 harmonic distortion limits, the designed filter is said to be compatible. Otherwise, filter is re-designed with new parameters to meet the IEEE 519-2014 distortion limits [352].

5.5 State Space Analysis

To have better understanding of the said problem, the system has been analysed using State Space Analysis. In fact, the state is an entity, described through a set of parameters. The state space analysis is widely used for determining the transient response of the network or system, but here our primary interest is to find the frequency response and also use of states space for analysis of resonance and design of filters. The state space representation describe physical system by a set of differential equations. The system transfer function of a network is a function of complex frequency 's'. System transfer function is the ratio of response to the excitation in Laplace transform. The examination of relationship between the state space and system transfer function is not discussed here, as it is out of the scope of this work.

There are many alternate ways of describing the behaviour of a dynamic system, using different state variables. State parameters are selected based on their physical significance. In the case of the simple R-L-C circuit, the inductor current and capacitor voltage are selected as state variables. These obviously has physical significance. The energy is stored in inductor is $\frac{1}{2}LI^2$, so, inductor current is selected as one state variable. Similarly, the capacitor energy is $\frac{1}{2}CV^2$, so, voltage across capacitor is taken as second state. At the resonance frequency, there will be continuous transformation of energy from electromagnetic form to electrostatic and vice-a-versa. This combination of state variables does make physical sense. In engineering, it is always preferred to formulate equations in terms of variables which has some physical significance. This has a number

of advantages, including the ability to make reality checks and providing us with an insight into the problem under study. There is a choice in the selection of state variables with physical significance. One can select either (flux ϕ , charge q) or (current i , voltage v) as preferred set of variables.

The single line diagram of network is given in figure (5.2). The complex network is simplified and reduced network for state space analysis is given in figure (5.3).

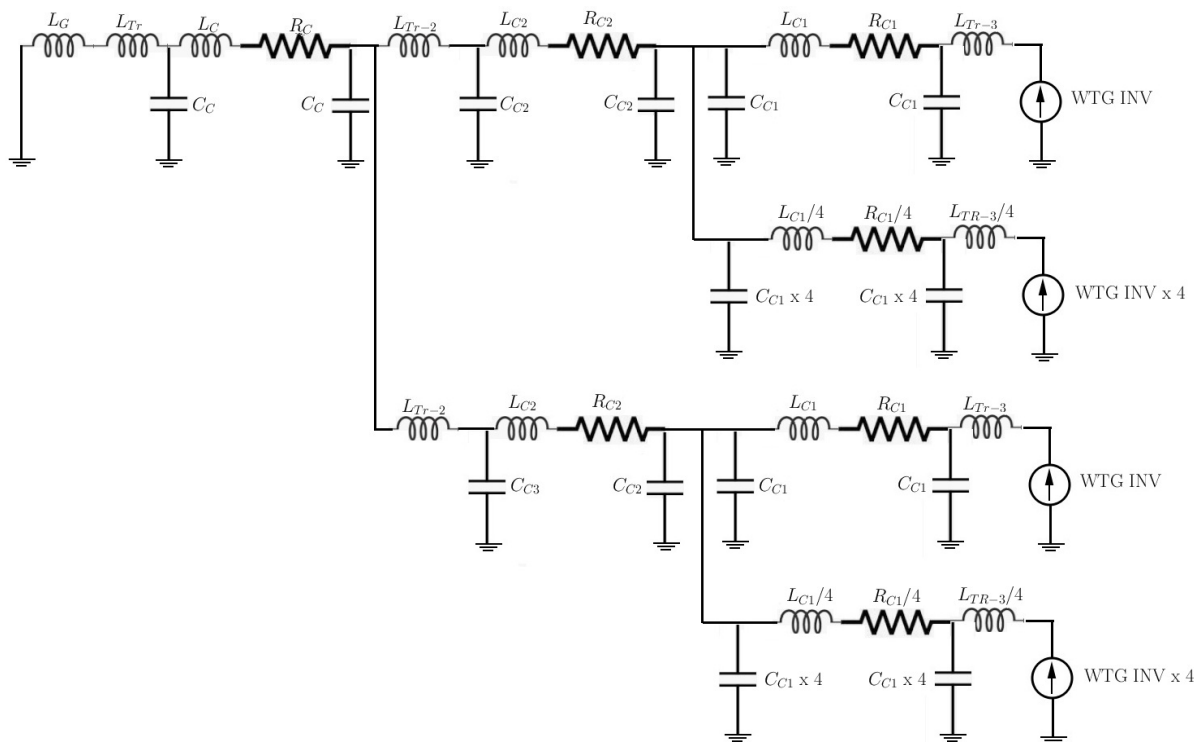


Figure 5.2: Single Line Diagram of System Network

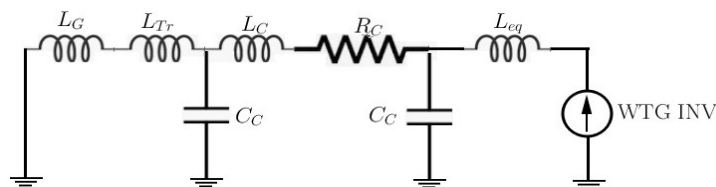


Figure 5.3: Simplified System Network

The state-space analysis of a linear network has been well accepted and widely used in power system analysis. It is the foundation for transient analysis of network. According

to this theory, the state variables of a linear network are the current of inductors and voltage of capacitors. A power system can thus be modelled as,

$$\dot{x} = Ax + Bu \quad (5.1)$$

Where, x is a state vector, A the state matrix, u the excitation / input vector and B is a contribution of input to the state variable. This equation can also be used to determine the transient response of a network. The solution of equation (5.1) is,

$$x(t) = x(0)e^{At} + \int_0^t e^{A(t-\tau)}Bu(\tau)d\tau \quad (5.2)$$

The eigenvalues of A , are called Eigenvalue of Modes of the system. Here, the reduced network of wind farm under study, has been analysed using the state-space method.

$$\begin{bmatrix} \dot{I}_1 \\ \dot{I}_2 \\ \dot{V}_1 \\ \dot{V}_2 \end{bmatrix} = \begin{bmatrix} -\frac{R_C}{L_C} & 0 & \frac{1}{L_C} & -\frac{1}{L_C} \\ 0 & 0 & 0 & \frac{1}{L_{TR}+L_G} \\ -\frac{1}{C_C} & 0 & 0 & 0 \\ \frac{1}{C_C} & -\frac{1}{C_C} & 0 & 0 \end{bmatrix} \begin{bmatrix} I_1 \\ I_2 \\ V_1 \\ V_2 \end{bmatrix} + \begin{bmatrix} 0 \\ 0 \\ \frac{1}{C_C} \\ 0 \end{bmatrix} [I_S] \quad (5.3)$$

Table 5.1: System Parameter

Sr. No	Parameter	Value
1	R_C	0.55 Ω
2	L_C	2.5 mH
3	C_C	0.3 μ F
4	L_{TR}	47 mH
5	L_G	0.3 mH
6	L_{Tr-2}	87.66 mH
7	C_{C2}	0.175 nF
8	L_{C2}	4.02 μ H
9	R_{C2}	0.07 Ω
10	L_{C1}	0.537 mH
11	R_{C1}	0.3072 Ω
12	C_{C1}	0.893 Ω
12	L_{Tr-3}	11.55 mH

The eigenvalues of the A are given below.

Table 5.2: Eigenvalues of Simplified Network

Sr. No	Eigenvalue	Natural Resonance Frequency (Order)
1	$-108.53 \pm 51986i$	165.4766 th
2	$-1.4817 \pm 59165i$	18.82 th

It is revealed from close analysis of eigenvalues of network, the first eigenvalue $-108.53 \pm 51986i$ is not very harmful to the system because of two reasons. First, the resonance frequency is very far away from the fundamental power frequency and also above the 50th order. Second, the real part of the eigenvalue is very high, which shows that, the transient will decay down very fast. The second eigenvalue, $-1.4817 \pm 59165i$, is lacking in both

aspects. First, the resonance frequency is below the 50th order and second, the real part is very small, which indicates the larger time of transient decay, so the transient will decay down very slowly.

The sensitivity of network element to the resonant frequency is given by the participation factors [359].

Table 5.3: Eigenvalue Sensitivity

Sr. No	State Variable	Sensitivity of mode 1 & 2	Sensitivity of mode 3 & 4
1	I_1	0.4933	0.0067
2	I_2	0.0067	0.4933
3	V_{C1}	0.2565	0.2434
4	V_{C2}	0.2434	0.2565

The highest participation factor shows the highest sensitivity of eigenvalues with respect to that state variable. Here, I_2 has the sensitivity of 0.4933, so, the effect of this state variable is highest in eigenvalues 3 & 4. Also, it is noteworthy that, the sensitivity values for eigenvalues 3 & 4 are same, as these are complex conjugate. The third and fourth large values are associated with state variables V_{C1} and V_{C2} , which are associated with the cable capacitance. The state variables and associated network parameters are given in the table (5.4). The participation of inductive and capacitive elements are exactly half of the total. The sum of participation of $L_1 = L_C$ and $L_2 = L_{TR} + L_G$ is 0.5 and that of C_1 and C_2 is also 0.5. The resonance is generated by only two elements, L & C, so the participation of each elements will be exactly half. Here, inductive elements L_1 , participates more in eigenvalue -1 & 2 (165.47th order), whereas L_2 is contributing more in eigenvalue- 3 & 4 (18.80th order).

Table 5.4: State Variable with Associated Network Parameter

Sr. No	State Variable	Associated Network Parameter
1	I_1	$L_1 = L_C$
2	I_2	$L_2 = L_{TR} + L_G$
3	V_{C1}	$C_1 = C_C$
4	V_{C2}	$C_2 = C_C$

The results are also verified using analytical method. The resonance frequency of the combination of variable with higher participation factor is calculated using,

$$f_{red} = \sqrt{\frac{1}{\omega^2 \times L_2 \times (C_1 + C_2)}} \quad (5.4)$$

According to Equation (5.4), the resonance frequency is of 18.80th order, which matches with the result of the space-space method. This proves the usability of state-space method for harmonic resonance analysis. The same analysis is done for eigenvalues 1 & 2. The results of analytical method and state space method are given in table (5.5).

Table 5.5: Comparison of State-Space and Analytical Method

Sr. No	State Space Method	Analytical Method
1	165.47	163.45
2	165.47	163.45
3	18.82	18.80
4	18.82	18.80

The state-space method has multifold benefits. First, it gives resonance frequencies of a network. Second, it is also useful in finding out the associated network parameter's contribution in a particular resonance frequency. So, without using complicated analytical

method or network reduction techniques, one can find the resonance frequency and also the method to reshape the frequency response. This can be utilized effectively in harmonic filter design.

5.6 Simulation of Harmonic Resonance of Network

With an extensive cable system, the capacitance of the cable can become a potential source of parallel resonance in the network. If the resonance is close to the dominant harmonic current components of the system loads, the harmonic current may get amplified and may lead to some failures in the system. Resonance occurs when the capacitive reactance of the cable and the inductive reactance of the system become equal. The frequency at which this occurs is referred to as the natural frequency for the system. This natural frequency depends on the system short circuit level and it varies with network configuration and change in the network. The resonant frequency decreases with increasing capacitance or with decreasing system short circuit level.

The Power Quality measurements done at site indicated that, there are significant 18th and 19th harmonics injected by the IGBT inverters. The resonance around this order can significantly increase voltage distortion levels and result into high voltage. To identify the natural frequency of the system, a frequency scan is performed on the network model, developed in previous section.

To carry out the simulation, first the inverter has been modelled as current source with fundamental current for active power generation and multiple other current source representing harmonic currents as per spectrum found in measurement. The other component of the network, transformers, transmission lines and cables, have been represented by their positive sequence impedance and admittance. The inverter is connected at 265 V level. After completion of modelling part, frequency scan has been done for wind power plant. The impedance plot for 33 kV WTG bus is shown in figure (5.4). It is the result of frequency scan for the 33 kV PCC. The scan shows that, resonance is around 18th harmonic order (910Hz). The plot itself indicates that, there is a harmonic component in voltage due to resonance effect at the frequency around 910Hz (18 times the fundamental frequency).

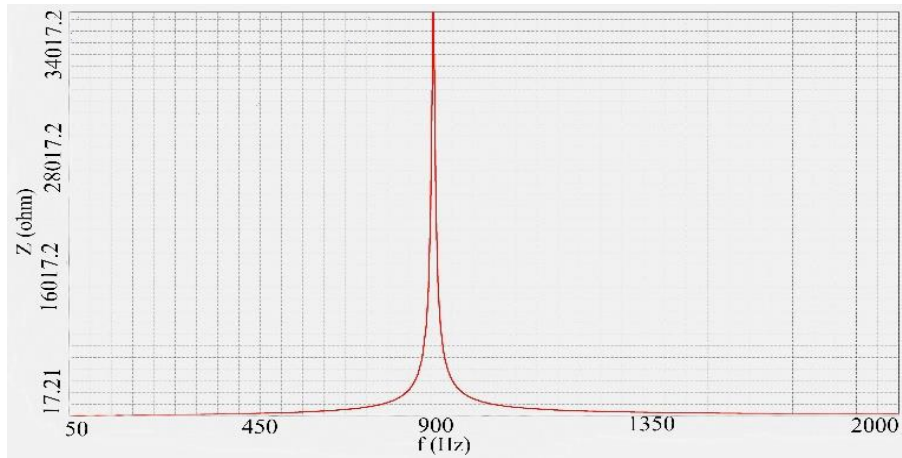


Figure 5.4: Impedance Plot for 33 kV WTG Bus

Further, the scan is performed at several buses (33 kV, 1.1KV & 0.265 kV) in the network and the voltage has been plotted to evaluate voltage behaviour of the network. As shown in figure (5.5) below, the voltage has been plotted against the time (for one cycle) for 33 kV PCC. The plot shows the harmonic overriding on fundamental voltage.

The simulated voltage for 33 kV bus shows the fundamental with high ripple voltage or distortion. The ripples were overriding on the fundamental voltage and increased the voltage up to 70 kV. Under normal condition, it should be around 46.5 KV ($33KV \times \sqrt{2}$), but due to distortion, the voltage was rising to 70 kV ($33KV \times \sqrt{2} \times 1.5$) as shown in figure (5.5). The ripples in the voltage may be attributed to the Asymmetrical Switching. As discussed earlier there is a change in IGBTs switching frequency. The positive and negative half cycle of PWM switching is not having symmetry and it exhibits as an additional ripples into voltage waveform. The hissing sound before tripping of inverter can be justified with the voltage waveform. Actually, inverters were trying to remain in synchronization with the grid voltage. As the grid voltage itself was distorted, the inverter was making fast switching of IGBT.

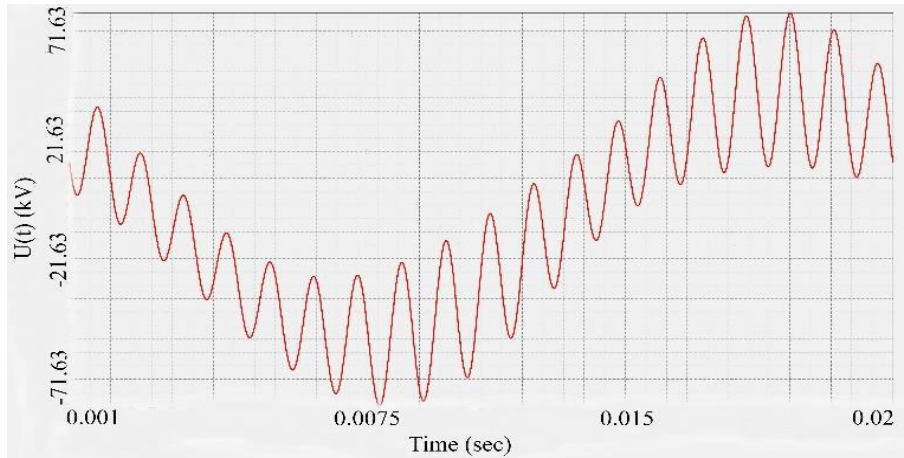


Figure 5.5: Voltage Plot for 33KV PCC

The plot for voltage harmonic spectrum is shown in figure (5.6). As the total distortion in voltage is high and exceeds IEEE 519-2014 distortion limits, the network should be analysed further for possibility of change in configuration or change in parameters. First, the attempt has been made to see the possibility to make change in contributing parameters. The eigenvalue- 3 & 4 are critical, as their frequency is less than 50th order and also it is affecting the operation of the wind power plant. The contributing parameters are cable capacitance and 33 kV/220 kV transformer reactance.

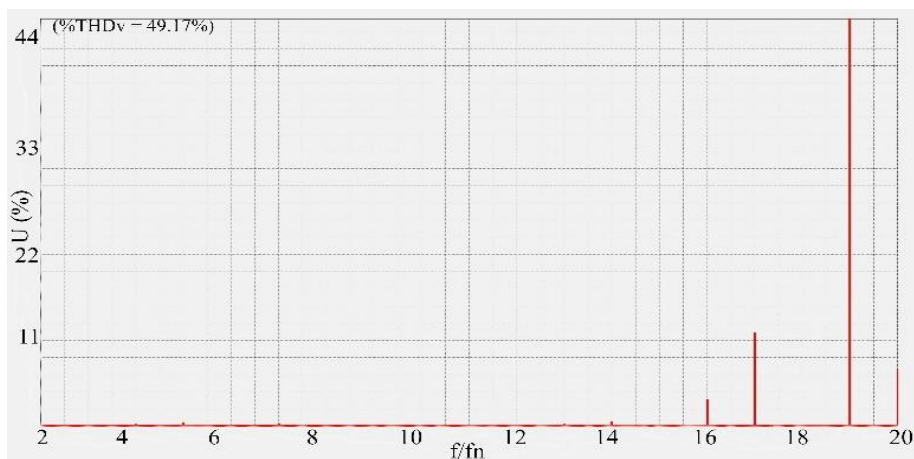


Figure 5.6: Voltage Harmonic Spectrum

Unfortunately, it is not possible to change or reconfigure both the elements. So, the next attempt is made for filter installation. So, the harmonics in the system should be mitigated by means of additional filtering equipment.

5.7 Harmonic Filter Design

A harmonic filter analysis was performed to investigate the potential filter configurations for reducing harmonic distortions. The harmonic filter has been considered for different locations.

From site measurement and also from simulation [358], it is concluded that the current distortion at individual bus is not exceeding, but the voltage distortion at 0.265 kV, 1.1 kV & 33 kV bus is exceeding the limits as per IEEE 519-2014. So, mitigation of harmonics is necessary to have the distortion limits within the allowable range.

This can be achieved using some additional Filtering Circuit. To design the Harmonic Filter, certain steps has been followed. The very first step is determination of the reactive power requirement for that particular bus. For that, Load Flow Analysis is a basic necessity.

5.7.1 Tuned Filter

After having multiple load flow results, the fundamental reactive power requirement is concluded for 0.265 kV, 1.1 kV and 33 kV voltage bus. After placing the multiple filters at different buses, % THD_V has been calculated at all buses. From all the results, the 1.1 kV bus, 100 kVAr passive harmonic filter was found relatively effective for the given system conditions. Several steps has been followed to design the 1.1 kV passive harmonic filter. The input data for filter design are $V=1.1$ kV, $Q=100$ kVAr, $f_n = 901.6$ Hz [360] [361] [362] [363].

The inductance of reactor of filter can be determined from following formula.

$$L = \frac{1}{(2\pi f_{res})^2 \times C} \quad (5.5)$$

It can be expressed in impedance in percentage using relationship between resonance frequency and impedance in percentage (%) [334].

$$f_{res} = \frac{50}{\sqrt{(X - L(\%) \times 100)}} \quad (5.6)$$

The inductive reactance is expressed in terms of the percentage of voltage drop occurs in series reactor, $X_L = nX_C$. The filter impedance can be determined from following

relation,

$$Z_{filter} = \frac{kV^2}{MVA_r} \quad (5.7)$$

The filter impedance is the difference of capacitive reactance and inductive reactance.

$$Z_{filter} = X_C - X_L \quad (5.8)$$

The inductive reactance is given in terms of percentage of capacitive reactance as given in equation (5.6). So, putting X_L in terms of X_C .

$$Z_{filter} = X_C - n \times X_C \quad (5.9)$$

$$X_C = \frac{Z_{filter}}{1 - n} \quad (5.10)$$

And X_L can be calculated from equation (5.11).

$$X_L = n \times X_C \quad (5.11)$$

The performance of LC tuned filter is also verified here using state-space method.

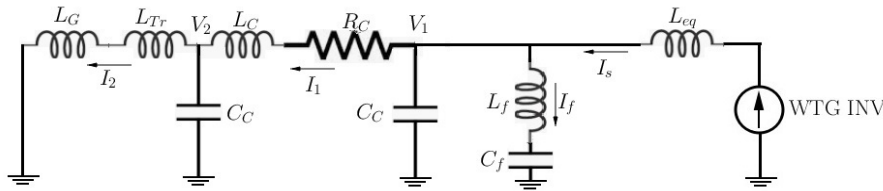


Figure 5.7: Network with LC Tuned Filter

The state space equations are given here.

$$\frac{dI_1}{dt} = -\frac{R_C}{L_C} I_1 + \frac{V_1}{L_C} - \frac{V_2}{L_C} \quad (5.12)$$

$$\frac{dI_2}{dt} = \frac{V_2}{(L_G + L_{Tr})} \quad (5.13)$$

$$\frac{dV_1}{dt} = \frac{I_S}{C_C} - \frac{I_1}{C_C} - \frac{I_f}{C_C} \quad (5.14)$$

$$\frac{dV_2}{dt} = \frac{I_1}{C_C} - \frac{I_2}{C_C} \quad (5.15)$$

$$\frac{dI_f}{dt} = \frac{V_1}{L_f} - \frac{V_{Cf}}{L_f} \quad (5.16)$$

$$\frac{dV_{Cf}}{dt} = \frac{I_f}{C_f} \quad (5.17)$$

These equations can be arranged and expressed in matrix form as given in equation (5.18).

$$\begin{bmatrix} \dot{I}_1 \\ \dot{I}_2 \\ \dot{V}_1 \\ \dot{V}_2 \\ \dot{V}_{Cf} \\ \dot{I}_f \end{bmatrix} = \begin{bmatrix} -\frac{R_C}{L_C} & 0 & \frac{1}{L_C} & -\frac{1}{L_C} & 0 & 0 \\ 0 & 0 & 0 & \frac{1}{L_{Tr}+L_G} & 0 & 0 \\ -\frac{1}{C_C} & 0 & 0 & 0 & 0 & -\frac{1}{C_C} \\ \frac{1}{C_C} & -\frac{1}{C_C} & 0 & 0 & 0 & 0 \\ 0 & 0 & 0 & 0 & 0 & \frac{1}{C_f} \\ 0 & 0 & \frac{1}{L_f} & 0 & -\frac{1}{L_f} & 0 \end{bmatrix} \begin{bmatrix} I_1 \\ I_2 \\ V_1 \\ V_2 \\ V_{Cf} \\ I_f \end{bmatrix} + \begin{bmatrix} 0 \\ 0 \\ \frac{1}{C_C} \\ 0 \\ 0 \\ 0 \end{bmatrix} [I_S] \quad (5.18)$$

The eigenvalues of the network with LC filter with $L_f = 104mH$ and $C_f = 0.3\mu F$ is given below.

Table 5.6: Eigenvalues with LC Filter

Sr. No	Eigenvalue	Natural Resonance Frequency (Order)
1	$-107.9 \pm 52137i$	165.95^{th}
2	$-2.09 \pm 4089i$	13^{th}
3	$-7.61e^{-3} \pm 8140.5i$	25.91^{th}

From eigenvalues given in table (5.6), the shift in resonant point can be seen after inclusion of LC Filter. In a bare network (i.e without LC Filter), there were two resonant frequencies. Now, with LC Filter, there are three resonant frequencies observed. Out of two resonant points, one resonant point does not get affected much by LC filter. However, the critical resonant point (i.e 18.80^{th}) is suppressed and two new resonant point (13^{th} and 26^{th}) is appeared. It is also verified using simulation and is given in result section. To avoid these problem, a C-Type Filter is evaluated here.

5.7.2 C-Type Filter

The C-type topology has been widely used in HVDC projects. The invention of C-type topology was made to avoid the 2^{nd} order harmonic resonance when 3^{rd} order tuned harmonic filter is used. This was a common problem observed in HVDC projects. As, the scope of this work is limited to the mitigation of 18^{th} order harmonic resonance and save inverters from tripping, and not the optimization of filter, the filter parameters are derived as suggested in [364].

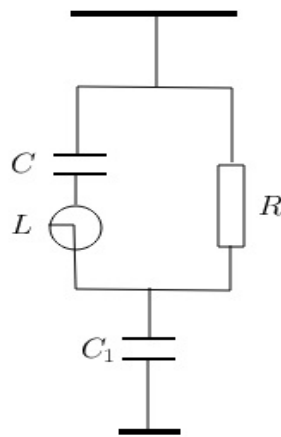


Figure 5.8: C-Type Topology

To determine the C- type filter parameter, the nominal voltage U_1 , tune frequency f_o , and the reactive power capacity Q_1 at fundamental frequency should be specified. Then, parameter L , C , and R can be determined using formulae derived here based on the analysis given in [364].

The filter impedance can be written as,

$$Z(\omega) = \left(\frac{1}{R} + \frac{1}{j\omega L - j(\omega C)^{-1}} \right) + \frac{1}{\omega C_1} \quad (5.19)$$

$$Z(\omega) = \frac{R(\omega^2 LC - 1)^2 + jR^2\omega C(\omega^2 LC - 1)}{(R\omega C)^2 + (\omega^2 LC - 1)^2} - j\frac{1}{\omega C_1} \quad (5.20)$$

L and C are tuned to fundamental power frequency, to avoid the power loss in R .

$$\omega_F^2 LC - 1 = 0 \quad (5.21)$$

So, the impedance is given by

$$Z = \frac{1}{j\omega C} = \frac{U_1^2}{j\omega C_1} \quad (5.22)$$

At tuned frequency, the imaginary part of filter impedance is zero and total impedance is purely resistive.

$$\frac{jR^2\omega_o C(\omega_o^2 LC - 1)}{(R\omega_o C)^2 + (\omega_o^2 LC - 1)^2} - j\frac{1}{\omega_o C_1} = 0 \quad (5.23)$$

and the total resistance is,

$$r = \frac{R(\omega_o^2 LC - 1)^2}{(R\omega_o C)^2 + (\omega_o^2 LC - 1)^2} \quad (5.24)$$

From equation (5.23) and (5.24), we can write,

$$\frac{\omega_o RC}{\omega_o^2 LC - 1} = \frac{1}{r\omega_o C_1} \quad (5.25)$$

Using equation (5.25), the equation (5.24) can be written as,

$$r = \frac{R}{\frac{1}{(r\omega_o C_1)^2} + 1} \quad (5.26)$$

re-arranging equation (5.26),

$$r^2 - Rr + \frac{1}{(\omega_o C_1)^2} = 0 \quad (5.27)$$

Where ω_o is resonance frequency. It is given by

$$\omega_o = \frac{1}{2\pi\sqrt{LC}} \quad (5.28)$$

and h_o is the harmonic order.

$$h_o = \frac{\omega_o}{\omega_F} \quad (5.29)$$

Assuming,

$$R_o = \frac{2}{(\omega_o C_1)} = \frac{2U_1^2}{h_o Q_1} \quad (5.30)$$

then, equation (5.27) can be re-written as,

$$r^2 - Rr + \frac{(R_o)^2}{4} = 0 \quad (5.31)$$

As already discussed, r is the resistance of filter at resonance frequency. Its value must be positive and real. This is only possible if following condition is satisfied.

$$r \geq R_o \quad (5.32)$$

Which can be satisfied if,

$$r = mR_o \quad (5.33)$$

Where, $m \geq 1$. Using this relation, equation (5.31) can be written as,

$$r^2 - mR_o r + \frac{(R_o)^2}{4} = 0 \quad (5.34)$$

The roots of equation (5.34) are

$$r = \frac{m \pm \sqrt{m^2 - 1}}{2} R_o \quad (5.35)$$

The value of r can be used in equation (5.21) and (5.25), the value of, parameter m , L and C of the filter can be derived from following two equations (5.36) & (5.37) [13].

$$C = \frac{h_o^2 - 1}{m^2 - m(\sqrt{m^2 - 1})} \times \frac{Q_1}{2U_1^2 \omega_F} \quad (5.36)$$

$$L = \frac{m^2 - m(\sqrt{m^2 - 1})}{h_o^2 - 1} \times \frac{2U_1^2}{Q_1 \omega_F} \quad (5.37)$$

By choosing an appropriate value of m , the parameters L , C , R and C_1 can be determined. The cost of the filter depends on the value of its components R , L , C and C_1 . The cost of filter can be minimized, if their capacities are reduced to a minimum. The minimum cost of the C-type filter is equal to the tuned filter, occurs at $m = \infty$. Generally, m is selected greater than 1. The different values of L & C are given in table (5.7) for different values of m .

Table 5.7: Filter Parameter for Different Value of Parameter m

Sr. No	m	L mH	C μF
1	2	105.2	96.3
2	3	101	100.3
3	4	99.70	101.6
4	5	99.1	102.2
5	10	98.4	102.98

To find out the resonant points of network with C-Filter, state-space analysis has been carried out. The simplified network with C-Filter is shown in figure (5.9). The state space equation of network with C-Type Filter has also been given here. It is important to note that, in C-Filter an additional inductor L_1 of very small value is introduced deliberately to

make balance matrix. It is required, as the eigenvalues are present in complex conjugate pair. So, very small value of L_1 does not affect the other eigenvalues.

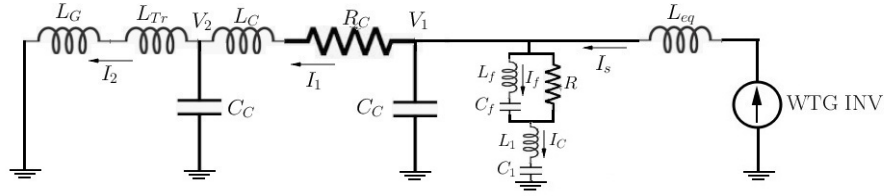


Figure 5.9: Network with C - Type Filter

$$\frac{dI_1}{dt} = -\frac{R_C}{L_C} I_1 + \frac{V_1}{L_C} - \frac{V_2}{L_C} \quad (5.38)$$

$$\frac{dI_2}{dt} = \frac{V_2}{(L_G + L_{Tr})} \quad (5.39)$$

$$\frac{dV_1}{dt} = \frac{I_s}{C_C} - \frac{I_1}{C_C} - \frac{I_C}{C_C} \quad (5.40)$$

$$\frac{dV_2}{dt} = \frac{I_1}{C_C} - \frac{I_2}{C_C} \quad (5.41)$$

$$\frac{dI_f}{dt} = \frac{I_C}{L_f} - \frac{I_f}{L_f} - \frac{V_{Cf}}{L_f} \quad (5.42)$$

$$\frac{dV_{Cf}}{dt} = \frac{I_f}{C_f} \quad (5.43)$$

$$\frac{dI_C}{dt} = \frac{V_1}{L_1} - \frac{I_C R}{L_1} + \frac{I_f R}{L_1} - \frac{V_{C1}}{L_1} \quad (5.44)$$

$$\frac{dV_{C1}}{dt} = \frac{I_c}{C_1} \quad (5.45)$$

These equations can be arranged and expressed in matrix form as given in equation (5.46).

$$\begin{bmatrix} \dot{I}_1 \\ \dot{I}_2 \\ \dot{V}_1 \\ \dot{V}_2 \\ \dot{V}_{Cf} \\ \dot{I}_f \\ \dot{V}_{C1} \\ \dot{I}_C \end{bmatrix} = \begin{bmatrix} -\frac{R_C}{L_C} & 0 & \frac{1}{L_C} & -\frac{1}{L_C} & 0 & 0 & 0 & 0 \\ 0 & 0 & 0 & \frac{1}{L_{TR}+L_G} & 0 & 0 & 0 & 0 \\ -\frac{1}{C_C} & 0 & 0 & 0 & 0 & 0 & 0 & -\frac{1}{C_C} \\ \frac{1}{C_C} & -\frac{1}{C_C} & 0 & 0 & 0 & 0 & 0 & 0 \\ 0 & 0 & 0 & 0 & 0 & \frac{1}{C_f} & 0 & 0 \\ 0 & 0 & 0 & 0 & -\frac{1}{L_f} & -\frac{R}{L_f} & 0 & \frac{R}{L_f} \\ 0 & 0 & 0 & 0 & 0 & 0 & 0 & \frac{1}{C_1} \\ 0 & 0 & \frac{1}{L_1} & 0 & 0 & \frac{R}{L_1} & -\frac{1}{L_1} & -\frac{R}{L_1} \end{bmatrix} \begin{bmatrix} I_1 \\ I_2 \\ V_1 \\ V_2 \\ V_{Cf} \\ I_f \\ V_{C1} \\ I_C \end{bmatrix} + \begin{bmatrix} 0 \\ 0 \\ \frac{1}{C_C} \\ 0 \\ 0 \\ 0 \\ 0 \\ 0 \end{bmatrix} \quad [I_S] \quad (5.46)$$

The value of C_1 is fixed at $0.3\mu F$, to get required reactive power at fundamental frequency. The other parameters of C - Type filter L , C and R are varied and the eigenvalues are checked to examine the suitability of filter. The value of parameter m is selected as 3 for sake of convenience. The eigenvalues for selected design ($L = 9.9mH$, $C = 10000\mu F$, and $C_1 = 3\mu F$) are given here.

Table 5.8: Eigenvalues with C-Type Filter

Sr. No	Eigenvalue	Natural Resonance Frequency (Order)
1	$-1.44859e^3 \pm 53572i$	170.50^{th}
2	$-1.289e^3 \pm 14912i$	47.46^{th}
3	$-8.511 \pm 2220i$	7^{th}
4	$-1.4023 \pm 0i$	0
5	$-6.95e^{12} \pm 0i$	0

The result of eigenvalue of network with C-Filter is shown in table (5.8). There are five distinct eigenvalues. Out of five different eigenvalues, two are non-oscillatory and one is near to fundamental frequency. One eigenvalue is 170.50^{th} is very high. The critical eigenvalue (18.80^{th}) is disappeared and one new frequency of 47.5^{th} order is appeared. It

is also under 50^{th} order, but harmonic current of this order is very low and its impact may not be significant. What is more, the damping factor is very high, so under transient condition it will decay very fast. There is one eigenvalue of low frequency (7^{th}), which is unlikely to affect the performance, as the inverter switching frequency is high and it does not produce current harmonics of low frequency. The steady state impact of C-Type filter is evaluated using simulation and is given in result and discussion section.

5.8 Results and Discussion

First, the series tuned filter topology is considered and the change in the system characteristics has been analysed. After having the 18^{th} order Single Tuned L-C Filter at 1.1KV bus, various parameters like the impedance, voltage and voltage spectrums are plotted. The Impedance which was earlier having peak around 940 Hz (18^{th} order) is shifted to the frequency around 1200 Hz (24^{th} order) as shown in figure (5.10). This result is somewhat in line with the state space analysis, which showed presence of resonance at around 26^{th} order. The differences in result of state-space analysis and simulation are due to the use of simplified network in state space analysis. However, it does not make any significant difference. The important point worth noting is that, the impedance at 18^{th} order is reduced to around 20Ω against the impedance (around $3.4\text{ k}\Omega$) of original network (without LC tuned Filter). The negative point of tuned filter is the shifting of harmonic resonance from around 18^{th} order to 24^{th} order, which is also under 50^{th} order and may cause the trouble. Though, the current harmonics of 24^{th} order was not present in the inverter output current, but it is possible that 24^{th} order may present under transient condition. As the time constant of circuit is very large and impedance at 24^{th} order is still large, even a small harmonic current will result in to slow decaying harmonic voltage, which may sustained for longer time and trip the inverter.

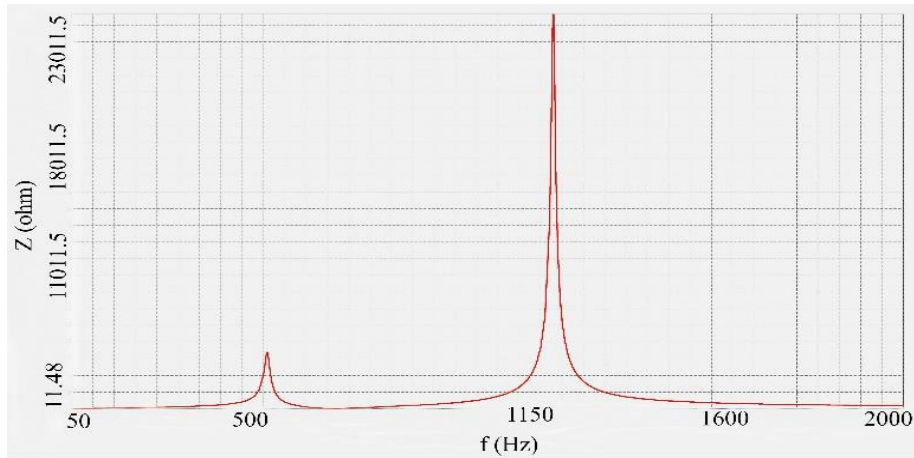


Figure 5.10: Shift in Resonance Frequency with Tuned LC Filter

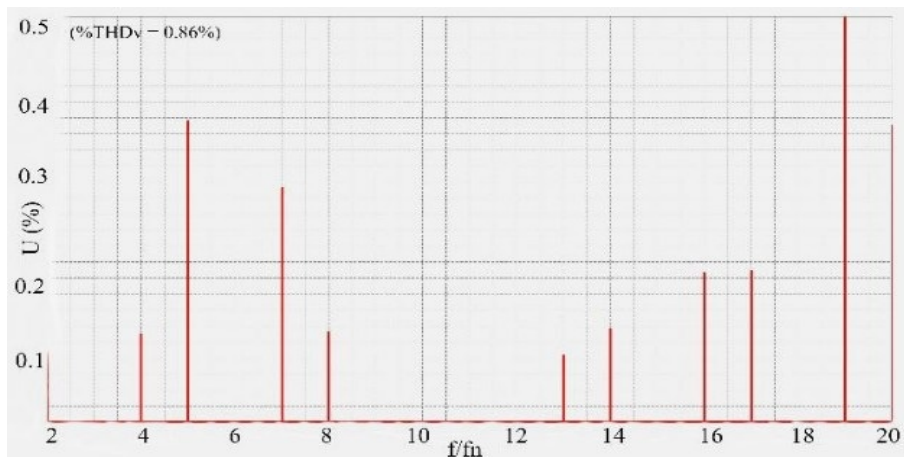


Figure 5.11: Frequency Spectrum with Tuned LC Filter

Though, the tuned filter is effective in curbing the harmonic resonance at 18^{th} order, but the resurgence of harmonic resonance at 24^{th} order may cause the problem. Though, there was almost negligible amount of current harmonics around 24^{th} order, but it may be generated during transient condition. This may cause slow decaying oscillatory transient of 24^{th} order. So, an effort is made to improve the performance of filter by using C-Type topology. The state space analysis of C-Filter is carried out. It shows that the harmonic resonance at around 47^{th} order, but its damping is very high. So, even in transient condition, if there are harmonics current of 47^{th} order it may decay very fast and will not result in long sustained high frequency oscillation ride on fundamental frequency. The frequency spectrum of below 20^{th} order is not much differ from that of network with *LC*

filter given in figure (5.11). The voltage waveform on 33 kV bus with C-Filter is given in figure (5.12).

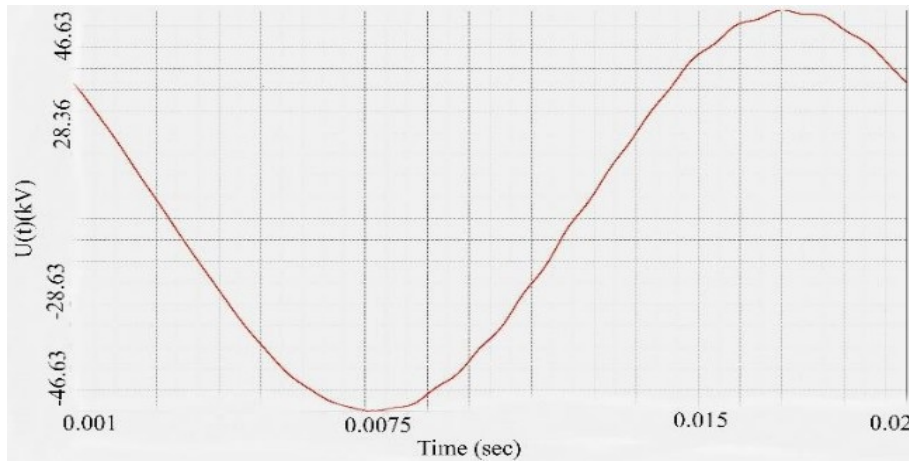


Figure 5.12: Voltage Waveform with C-Type Filter

The voltage waveform as shown in figure (5.12) is free from high frequency harmonics. So, C- Filter can be installed at 33 kV bus to effectively solve the problem of harmonic resonance.

5.9 Conclusion

In this chapter, a real case of inverter malfunction at wind power plant has been presented. This case shows the inverter's dependency on the power system network. Even with the small amount of current harmonic, the system voltage may get affected due to harmonic resonance. Also, the case presents practical difficulties in selection of filter design. Any change in network may lead to the change in network resonance point and may render installed filter unsuitable. In the presented case, the possibility of changes in network was limited and thus the problem of filter design was not as complicated as it would have been with complex network. The designed filter was installed at site and the performance was monitored during performance contract period and no tripping was observed. It can be inferred from this case that the cable length and transformer impedance are very important from harmonic stability point of view. If it is not properly taken in to account during planning stage, it may hamper the smooth performance of grid connected inverter. This makes filter installation mandatory for grid connected wind turbine (type-3 and

type-4). The filter characteristics also gets affected by the type of inverter controller and controller parameters. Performance of different types of inverter output filters and effect of inverter control parameters on output impedance of converter has already been discussed in chapter 4.